Scaling Shear Modulus from Small to Finite Strain for Unsaturated Soils

Yi Dong, Ph.D., A.M.ASCE[1]; Ning Lu, Ph.D., F.ASCE[2]; and John S. McCartney, Ph.D., P.E., M.ASCE[3]

Abstract: The stress-dependent curve of shear modulus degradation with increasing shear strain amplitude is a fundamental mechanical property of soils. Although it is well known that the degree of saturation has an important impact on the small strain shear modulus of unsaturated soils, its role on the shear modulus evolution with strain has not been thoroughly investigated. A testing program has revealed strong correlations between two key parameters of the shear modulus degradation curve, the reference strain and the coefficient of curvature, and parameters of the soil water retention curve (SWRC). An SWRC model capable of distinguishing between soil water in the capillary and adsorption regimes was used to correlate the reference strain to the maximum adsorption water content and pore size distribution of a soil, and to correlate the curvature coefficient to the maximum adsorption water content. A hyperbolic equation for the shear modulus reduction curve using these correlations shows good performance in predicting the shear modulus under unsaturated small or finite strain conditions. The new model was validated using the shear modulus reduction curve of independent data sets measured at different shear strains. **DOI: 10.1061/(ASCE)GT.1943-5606.0001819.** © *2017 American Society of Civil Engineers.*

Author keywords: Small strain shear modulus; Shear modulus reduction; Bender elements; Soil water retention; Suction stress; Unsaturated soils.

Introduction

The degradation in shear modulus of soils with increasing shear strain amplitude has a significant impact on the design and analysis of a wide range of geotechnical engineering applications, such as deep excavations, soil-structure interaction, and the dynamic response of soils under seismic loading (Viggiani and Atkinson 1995; Kramer 1996; Rampello et al. 1997; Clayton 2011; Likitlersuang et al. 2013; Yang and Gu 2013). Experimental studies on the relationship between shear modulus reduction and shear strain have found that the strain-related shear modulus varies greatly depending on soil type, plasticity index, initial density or void ratio, stress history or overconsolidation ratio (OCR), loading cycles and frequencies, and soil degree of saturation (Hardin and Drnevich 1972a, b; Iwasaki et al. 1978; Kokusho 1980; Yokota et al. 1981; Seed et al. 1986; Idriss 1990; Vucetic and Dobry 1991; Ishibashi and Zhang 1993; Borden et al. 1996; Darendeli 2001; Alramahi et al. 2008; Khosravi and McCartney 2012). In particular, the evolution of shear modulus with increasing shear strain amplitude for unsaturated soils is affected by both environmental loading (e.g., changes in relative humidity or matric suction) and stress state (e.g., effective stress and suction stress) (Dong et al. 2016; Dong and Lu 2016a). However, the coupling between the strain-dependency of the shear modulus reduction and the hydraulic properties of unsaturated soils has not been thoroughly studied. This is partially due to the fact that several different soils that have different shear modulus reduction curves and hydraulic properties should be investigated in order to delineate correlations.

A typical strain-hardening shear stress-strain relationship of a soil is shown in Fig. 1, which reflects a nonlinear increase in shear stress as the shear strains develop in the soil, with a gradual descending rate of increase until the soil reaches its peak shear strength (e.g., Viggiani and Atkinson 1995; Atkinson 2000). In other words, the ratio of shear modulus at any shear strain to the maximum shear modulus decreases with increasing shear strain. The relationship between normalized shear modulus, G/G_{max}, and shear strain, γ, is often referred to as the shear modulus degradation curve or the shear modulus reduction curve. When the shear strain amplitude is very small (usually less than 0.001%), the stress-strain relationship can be considered linear elastic. In the small strain range, the shear strains in the soil primarily occur due to particle oscillation under the propagation of elastic stress waves, and do not lead to changes in the soil structure or fabric (Santamarina et al. 2001). Hence, the slope at this strain range for a given stress state can be defined as the maximum, initial, or small strain shear modulus, defined with either the symbols G_{max} or G_0. On the contrary, as the shear strain increases beyond the soil-specific cyclic threshold shear strain, the soil will incur permanent deformations under static or cyclic loading. In this case, soil particles may rearrange their positions and change the numbers of contacts to adjust to the stress redistribution. Most soils will be at a strain level greater than the cyclic threshold shear strain by a shear strain of 1%, therefore this strain level is referred to in this study as being representative of finite strains (i.e., larger than small strains but still small with

[1]Associate Professor, State Key Laboratory of Geomechanics and Geotechnical Engineering, Institute of Rock and Soil Mechanics, Chinese Academy of Sciences, Wuhan, Hubei 430071, P.R. China; formerly, Dept. of Civil and Environmental Engineering, Colorado School of Mines, Golden, CO 80401 (corresponding author). ORCID: https://orcid.org/0000-0003-1237-0079. E-mail: ydong@whrsm.ac.cn

[2]Professor, Dept. of Civil and Environmental Engineering, Colorado School of Mines, 1012 14th St., Golden, CO 80401. E-mail: ninglu@mines.edu

[3]Associate Professor, Dept. of Structural Engineering, Univ. of California San Diego, La Jolla, CA 92131. E-mail: mccartney@eng.ucsd.edu

Note. This manuscript was submitted on July 28, 2016; approved on July 21, 2017; published online on December 5, 2017. Discussion period open until May 5, 2018; separate discussions must be submitted for individual papers. This paper is part of the ***Journal of Geotechnical and Geoenvironmental Engineering***, © ASCE, ISSN 1090-0241.

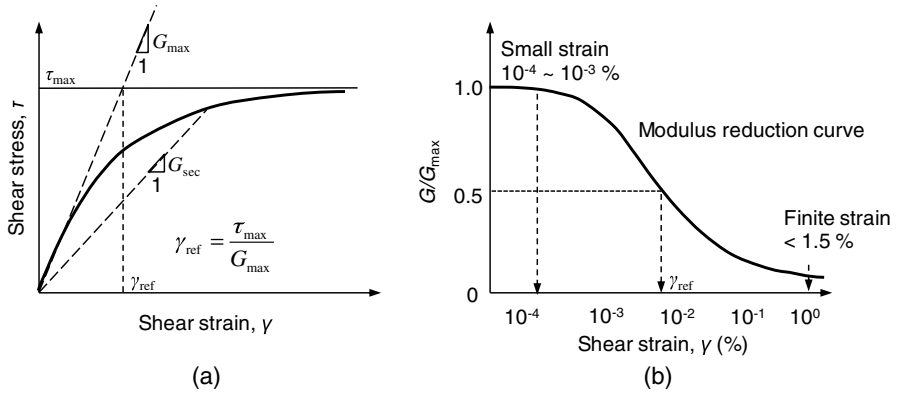

Fig. 1. (a) Typical shear stress-strain relationship; (b) shear modulus degradation with increased strain magnitude for a strain-hardening material

respect to strain required to reach failure in the backbone shear stress-strain curve). Accordingly, the shear modulus at this larger shear strain of 1% is referred to as the finite strain shear modulus, G_1 (e.g., Lu and Kaya 2014).

Although the degradation behavior of shear modulus with increasing shear strain is well recognized, the complexities of this shear modulus degradation dependence on compaction conditions and stress states still cannot be fully captured by existing models. For unsaturated soils, the mechanical properties are significantly affected by the relationships governing soil water retention and interparticle stresses, which are coined the soil water retention curve (SWRC) and suction stress characteristic curve (SSCC), respectively. In this study, the shear moduli at small strain levels, G_{max}, and finite strain levels, G_1, for a wide range of soils having different volumetric water contents are compared and investigated. A conceptual model previously developed by the authors is then extended to form a generalized empirical model capable of describing the strain dependency of shear modulus of unsaturated soils. The correlation between the proposed shear modulus reduction behavior and SWRC of soils reveals the effects of different regimes of soil water on patterns of shear modulus degradation for different types of soil at various degrees of saturation.

Mechanisms of Shear Modulus Strain-Dependency

Existing Shear Modulus Reduction Models

In order to describe the nonlinear shear stress-strain relationship of soils, a number of mathematical models have been proposed by different researchers to capture the features of shear modulus reduction curve. Table 1 provides four typical equations using a hyperbola to represent the shape of the curve, each containing 1–3 parameters. Hardin and Drnevich (1972b) introduced a reference strain, γ_{ref}, to normalize the already dimensionless strain quantity for better investigation of the stress-strain behavior. The reference strain is defined as the ratio between maximum shear stress and the maximum shear modulus: $\gamma_{ref} = \tau_{max}/G_{max}$, and the shear stress-strain relationship was formulated as follows:

$$\tau = \frac{\gamma}{\frac{1}{G_{max}} + \frac{\gamma}{\tau_{max}}} = \tau_{max}\frac{\gamma}{\gamma_{ref} + \gamma} \tag{1}$$

where τ and γ = shear stress and shear strain, respectively. Substituting the definition of the shear modulus ($G = \tau/\gamma$), a hyperbolic equation can be further derived from Eq. (1) to represent the ratio G/G_{max} as a function of shear strain, as follows:

$$\frac{G}{G_{max}} = \frac{1}{1 + (\frac{\gamma}{\gamma_{ref}})} \tag{2}$$

In this representation, the shear modulus decreases to half of its maximum value as the shear strain increases from zero to the reference strain, γ_{ref}, as shown in Fig. 1. However, this single-parameter model fails to fully capture the variation of the shape of the reduction curve caused by different factors such as the OCR or mean effective stress. This suggests that the reference strain varies depending on the stress state and type of soil.

To address this issue, Yokota et al. (1981) formulated an alternative expression for the modulus reduction curve that does not use a reference strain by including a power law function of the shear strain, γ, with α and β being empirical parameters, as follows:

$$\frac{G}{G_{max}} = \frac{1}{1 + \alpha\gamma^{\beta}} \tag{3}$$

Borden et al. (1996) modified this model by adding a third parameter to investigate the effect of cyclic loading on normalized shear modulus and damping ratio of different types of soils under various confining stresses. In the models of Yokota et al. (1981) and Borden et al. (1996), the empirically fitted parameters lack solid physical meaning, and are difficult to determine through experimental testing programs.

Darendeli (1997, 2001) proposed a modified hyperbolic equation based on the model of Hardin and Drnevich (1972b) to quantify the shear modulus reduction curve, using the reference strain, γ_{ref}, to better represent the nonlinearity in the relationship for soils under various stress states. The model is as follows:

$$\frac{G}{G_{max}} = \frac{1}{1 + \left(\frac{\gamma}{\gamma_{ref}}\right)^{m}} \tag{4}$$

Table 1. Existing Models for Shear Modulus Reduction

Reference	Model	Parameters
Hardin and Drnevich (1972b)	$\frac{G}{G_{max}} = \frac{1}{1 + (\frac{\gamma}{\gamma_{ref}})}$	γ_{ref}
Yokota et al. (1981)	$\frac{G}{G_{max}} = \frac{1}{1 + \alpha\gamma^{\beta}}$	α and β
Borden et al. (1996)	$\frac{G}{G_{max}} = \frac{1}{1 + (a \cdot \gamma^{b})^{c}}$	a, b, and c
Darendeli (2001)	$\frac{G}{G_{max}} = \frac{1}{1 + (\frac{\gamma}{\gamma_{ref}})^{m}}$	γ_{ref} and m

where m = constant that represents the curvature of the modulus reduction curve. In this equation, the reference strain controls the location where G decreases to half of its maximum value as the shear strain increases. In other words, m reflects the rate of decrease in G with shear strain. This two-parameter-type hyperbolic model still has a simple form with sufficient accuracy to capture the shape of the modulus reduction curve and evolution with different variables over a wide range of strain magnitudes. In the development of the new model, a two-parameter equation is proposed building on the equation of Darendeli (1997, 2001) in which the physical meaning of the parameters is investigated to consider the effect of varying initial volumetric water content of unsaturated soils.

Scaling from Small Strain to Finite Strain

Although the effects of mean effective stresses and OCR on the shear modulus reduction curves of saturated or dry soils have been widely explored using torsional shear or simple shear tests (e.g., Yokota et al. 1981; Ishibashi and Zhang 1993; Borden et al. 1996), fewer studies have been performed for unsaturated soils (e.g., Kim et al. 2003; Hoyos et al. 2015; Suprunenko and Ghayoomi 2015). The shear modulus degradation behavior for unsaturated soils and its dependency on soil type needs further investigation. Lu and Kaya (2013) used the drying cake method to measure the Young's modulus of soil under partially saturated conditions obtained using static loading to a shear strain of approximately 1%, and found that it is related to the volumetric water content of the soil through a power law relationship. They found that at this finite strain level, the stiffness of the material is gained from the combined stiffness of the particle and liquid components. Further, as the volumetric water content of soil decreases, the lubricating effect of water on the soil particle interaction diminishes. Dong et al. (2016) applied the relationship defined for the finite strain modulus by Lu and Kaya (2014) to the small strain shear modulus of soils to consider the impacts of the degree of saturation and the particle contact forces defined via the suction stress-based effective stress. At small strains, the stiffness of the soil skeleton arises due to particle hydration, and the stiffness is enhanced by contact forces throughout the particle networks due to the capillarity and adsorption water, which can be characterized by the suction stress.

Fig. 2 illustrates the mechanisms influencing the small strain and finite strain shear moduli values. Recent advances in soil science allow a clear separation of the soil water interaction into regimes of capillary water and adsorptive water (e.g., Or and Tuller 1999; Frydman and Baker 2009; Revil and Lu 2013; Tuller et al. 1999). Accordingly, two mechanisms attributed to the scaling effect of shear modulus variations with shear strain were proposed to represent the effect of material stiffness in a soil matrix or particle clusters and the effect of contact forces. In the capillary water regime shown in Fig. 2(a), the contact force is developed by the surface tension due to the presence of the air-liquid interfaces. As the water content decreases, the contact force or suction stress increases with higher curvature of the interfaces. In the adsorption water regime shown in Fig. 2(b), the magnitude of particle attraction due to van der Waals attraction or Coulomb forces is much higher than that due to capillary attraction (Lu and Likos 2004; Lu and Khorshidi 2015). This indicates that the small strain shear modulus increases by a larger amount and at a greater rate than the finite strain shear modulus as the soil dries.

Following on the conceptual model in Fig. 2, a modified effective stress term, $\alpha \times \sigma'$, is introduced to remove the effect of stress state on the reference strain, so that the value of the reference strain in the shear modulus reduction curve can be considered as a material property that only depends on soil type and degree of saturation. This new term was incorporated into the shear modulus reduction curve of Darendeli (2001) to define a new shear modulus reduction curve as follows:

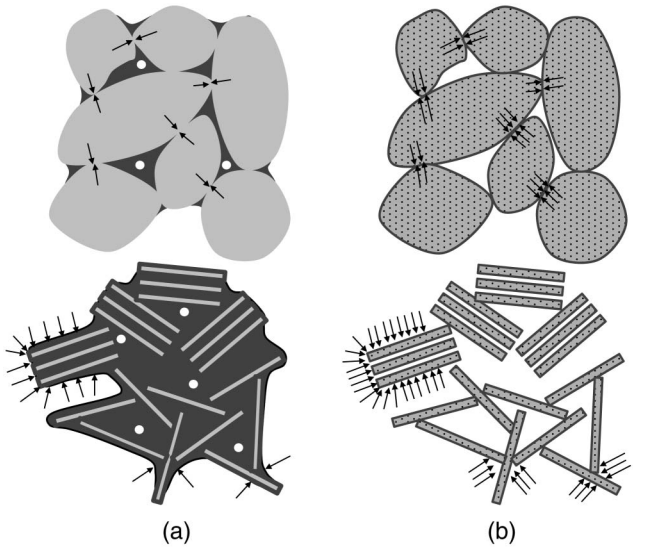

Fig. 2. Illustration of the effects of soil moisture on the magnitude of shear modulus: (a) capillary water regime; (b) adsorption water regime

$$\frac{G}{G_{\max}} = \frac{1}{1 + \left[\frac{\gamma}{(\alpha\sigma')\gamma_{\text{ref}}}\right]} \tag{5}$$

where α = inverse of the air-entry suction (1/kPa); and σ' = mean effective stress defined using the suction stress principle, as follows:

$$\sigma' = \sigma - \sigma^s \tag{6}$$

where σ and σ^s = mean total stress and suction stress, respectively. The values of α and σ' are related to the shape of the SWRC, which will be discussed in a subsequent section. The parameters γ_{ref} and m in Eq. (5) are different than those in the model of Darendeli (2001) because the stress-state effects have been isolated.

Measured Soil Water Retention and Shear Modulus of Different Soils

SWRC of Soils Tested

This study investigated several remolded soils, which were pulverized after being oven dried before specimen preparation. The soil types considered range from sand and silt, to expansive clay and nonexpansive clay, as provided in Table 2. Soil specimens were compacted statically using a loading frame into circular, thin cakes having a diameter of 76.2 mm and a thickness of approximately 20 mm. The matric suctions in the specimens were inferred using the transient water release and imbibition method (Wayllace and Lu 2012) for the high water content range (above ~40% degree of saturation), and the vapor adsorption isotherm technique (Likos et al. 2011) for the medium to high suction range (above ~1,000 kPa). During the drying process, the evaporation rate was limited to ensure uniform water distribution within the soil cakes. The variations of sample volume were monitored by digital image analysis. Experimental details were elaborated in Lu and Kaya (2013)

Table 2. Test Soils and Classification, SWRC Parameters by the Lu (2016) Model, and Parameters for Correlations between Shear Modulus Degradation Characteristics and SWRC by the Empirical Fittings

Soil	USCS	Porosity (ϕ)	Correlation			Lu SWRC model parameters			
			m	ξ	η	α	N	θ_a^{max}	M
Esperance sand[a]	SP	0.39	1.141	−0.342	0.0026	0.220	2.520	0.010	0.009
Bonny silt[a]	ML	0.47	1.423	1.857	0.0027	0.091	1.531	0.024	0.058
Hopi silt[a]	SC	0.48	1.513	1.416	0.0059	0.046	1.742	0.063	0.122
BALT silt[a]	ML	0.47	1.580	2.086	0.0028	0.059	1.726	0.024	0.127
Iowa silt[a]	ML	0.45	1.609	1.195	0.0067	0.083	1.654	0.046	0.101
Denver claystone[a]	CL	0.55	1.656	2.974	0.0113	0.010	1.560	0.111	0.076
Denver bentonite[a]	CH	0.53	1.997	3.063	0.0159	0.014	1.410	0.156	0.196
Georgia kaolinite[a]	CL	0.58	1.762	−0.301	0.0082	0.011	2.350	0.070	0.010
Silty sand[b]	SM	0.42	1.705	2.612	0.0081	0.058	1.436	0.075	0.033
Subgrade soil[c]	SP	0.40	1.183	0.766	0.0019	0.015	2.056	0.009	0.007
Ottawa F75[d]	SW	0.30	1.339	−0.630	0.0027	0.214	2.525	0.017	0.003

Note: USCS = unified soil classification system.
[a]Data from Dong and Lu (2016a), test conducted by using drying and wetting cake technique.
[b]Data from Hoyos et al. (2015), test conducted by suction-controlled resonant column technique.
[c]Data from Kim et al. (2003), test conducted in a torsional resonant column system.
[d]Data from Suprunenko and Ghayoomi (2015), measured in a strain-controlled cyclic triaxial testing device.

and Dong and Lu (2016a). The results of previous experimental measurements of matric suction were then fitted using the new SWRC defined by Lu (2016). The SWRC of Lu (2016) can be expressed by the amount of different types of soil water in equilibrium with the soil suction or potential energy of soil water, evaluated using the following expressions:

$$\theta(\psi) = \theta_a(\psi) + \theta_c(\psi) \tag{7}$$

$$\theta_a(\psi) = \theta_a^{max}\left\{1 - \left[\exp\left(1 - \frac{\psi_{max}}{\psi}\right)\right]^M\right\} \tag{8}$$

$$\theta_c(\psi) = \frac{1}{2}\left[1 - \text{erf}\left(\frac{\psi - \psi_{cav}}{\sqrt{2}\delta_{cav}}\right)\right][\theta_s - \theta_a(\psi)][1 + (\alpha\psi)^N]^{1/N-1} \tag{9}$$

where ψ = matric suction (kPa); N = pore size distribution parameter in the van Genuchten (VG) SWRC model (van Genuchten 1980); and θ_a and θ_c = volumetric water content values corresponding to the limits of the adsorptive and capillary water ranges in Fig. 2, respectively. The SWRC model of Lu (2016) consists of a modified Freundlich-type model for adsorption [Eq. (8)] and a VG-type model for capillarity [Eq. (9)]. Eqs. (7)–(9) provide a quantitative assessment of the adsorptive water by a maximum adsorption water content, θ_a^{max}, and an adsorption strength parameter, M. The SWRC model of Lu (2016) also introduced maximum matric suction, ψ_{max}, and cavitation suction, ψ_{cav}, as two important controlling points to describe the soil water characteristic curves. In Eq. (9), a cumulative probability function $1/2\{1 - erf[(\psi - \psi_{cav})/(\sqrt{2}\delta_{cav})]\}$ with the standard normal distribution of the cavitation pressure $N(\psi_{cav}, \delta_{cav})$ was used to quantify the statistic uncertainty of the onset of capillary cavitation. According to Lu and Likos (2006), the suction stress can be conceptually defined as

$$\sigma^s(\theta) = \sigma_{pc}^s(\theta) + \sigma_c^s(\theta) \tag{10}$$

where σ_{pc}^s = component induced by physicochemical interaction of adsorption water (otherwise known as σ_a^s), and σ_c^s = component induced by capillary water. Recognizing that most experimental data used in this study are for matric suction within the capillary regime as the adsorptive suction stress component is not well established yet, the current study focuses on scaling of shear strain modulus within the capillary regime. Thus, the suction stress induced by matric suction in the capillary regime can be approximated by using an effective degree of saturation concept (Lu and Likos 2006; Lu et al. 2010), and is formulated as follows:

$$\sigma^s \cong \sigma_c^s = -S_e\psi = -\frac{\theta_c}{\theta_s - \theta_a}\psi = -\frac{\theta - \theta_a}{\theta_s - \theta_a}\psi \tag{11}$$

A typical SWRC quantification of the Lu (2016) model with the separation of capillary water and adsorptive water of Hopi silt is shown in Fig. 3. The SWRC model of Lu (2016) provides an excellent fit to the sigmoidal-shape development of capillary water at medium and low suction range and the wavy behavior of adsorptive water at high suction range. The fitted results show that Hopi soil reaches a maximum matric suction of 1,200 MPa with a cavitation suction of 25 MPa at the point where capillary attraction diminishes, and that Hopi silt possesses a maximum adsorption water content of 0.08. The calculated suction stress using Eq. (11) shows that Hopi silt develops suction stresses having magnitudes ranging from a few kPa at saturated conditions to approximately 100 kPa at dry conditions. The fitting parameters for all soils tested are provided in Table 2.

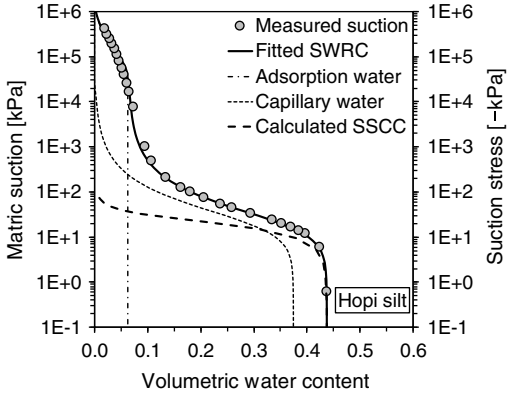

Fig. 3. Measured soil suction and typical SWRC and SSCC represented by Lu (2016) model for Hopi silt following a drying path

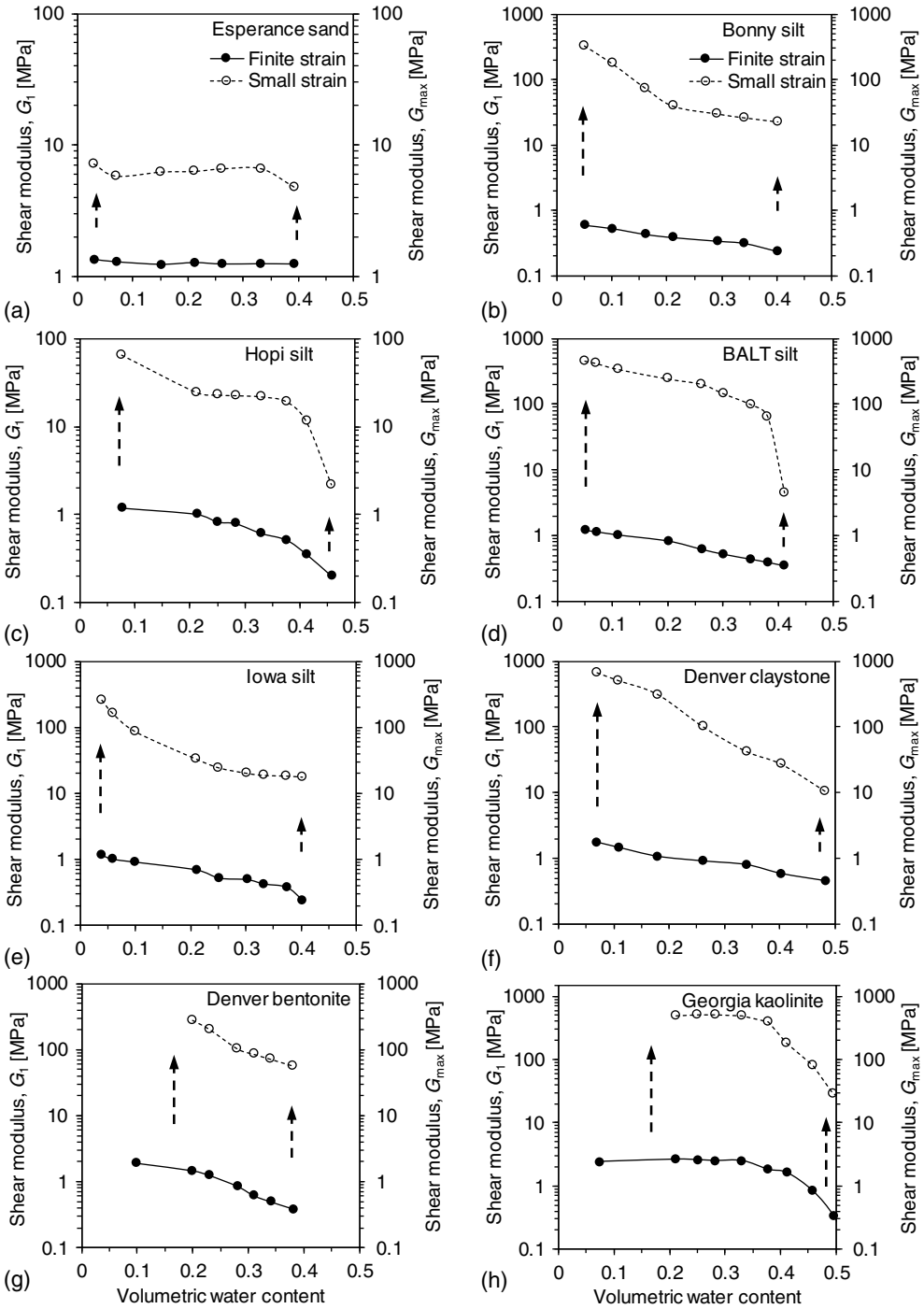

Fig. 4. Comparisons of shear modulus measured at finite-strain, G_1, and small-strain, G_{max}: (a) Esperance sand; (b) Bonny silt; (c) Hopi silt; (d) BALT silt; (e) Iowa silt; (f) Denver claystone; (g) Denver bentonite; (h) Georgia kaolinite

Comparison of G_{max} and G of the Soils Test

The finite strain shear moduli, G_1, of eight tested soils were converted from their Young's moduli assuming a Poisson's ratio of 0.25 obtained from static loading tests that did not cause irreversible plastic deformation (Lu and Kaya 2013). The small strain shear moduli, G_{max}, of these soils were calculated from shear wave velocities measured using the bender element technique (Dong and Lu 2016a, b). Comparisons of the small strain and finite strain shear modulus for the eight soils are shown in Fig. 4. The general trend shows that both finite strain and small strain shear moduli increase as the water content decreases, but following different patterns. The magnitude of finite strain modulus is always lower than the small strain modulus. The overall finite strain shear modulus increases slightly from sandy soil to silty and clayey soil but generally remains less than 2 MPa, whereas the small strain shear modulus shows significant difference from sandy soil to silty or clayey soil. The variation of G_{max} from saturated condition to dry condition can be in the same order of magnitude as the finite strain modulus for sandy soil (e.g., 4–7 MPa for Esperance sand) and with little increment as the soil dries. However, G_{max} for silty and clayey soil can increase in magnitude up to tens or hundreds of MPa as the soil dries [e.g., 2–65 MPa for Hopi silt, 18–257 MPa for Iowa silt,

J. Geotech. Geoenviron. Eng., 2018, 144(2): 04017110

23–328 MPa for Bonny silt, and 5–460 MPa for bay area landslide tasks (BALT) silt]. When the soil contains a higher clay content, which is reflected by the value of the maximum adsorption water content parameter, G_{max} can increase significantly from wet to dry conditions. For instance, G_{max} for Denver claystone increases up to 660 MPa as the volumetric water content decreases to 0.08. Georgia kaolinite shows an exceptional pattern from other expansive clays but resembles a similar shape of sandy soil like Esperance sand. Although G_{max} increases greatly as the Georgia kaolinite dries to a medium degree of saturation and it has significantly larger value of the modulus comparing to finite strain shear modulus, both Esperance sand and Georgia kaolinite show a plateau for degrees of saturation in the range of 0.2–0.8.

The preceding observation can be further explained by the proposed conceptual model. The stiffness of the soil matrix or particle clusters mainly contributes to the shear modulus at finite strain; whereas the contact force mechanism contributes to the shear modulus at small strains as the the soil dries. Capillary and adsorption water interactions play different roles in the contact force enhancement. The comparison of finite strain and small strain shear moduli of these eight soils can be grouped into three categories: sandy soils with little adsorption water and relatively large pore size thus weak capillarity (e.g., Esperance sand); silty soils and expansive clayey soils with considerable amount of adsorption water and relatively small pore size hence strong capillarity (e.g., Bonny silt, Hopi silt, BALT silt, and claystone); and nonexpansive clays which possess little adsorption water but small particle size therefore strong capillary effect (e.g., Georgia kaolinite). The contact force enhancement due to capillary effect results in small strain shear modulus with orders of magnitude higher than for finite strain shear modulus, but with fairly similar patterns. The stronger the capillary effect, the more prominent the enhancement (e.g., comparison between Esperance sand and Georgia kaolinite). The adsorption water does not contribute too much to the contact force or suction stress (Lu et al. 2010), but the crystalized water molecule structure formed by adsorptive interaction provides additional stiffness other than contact force enhancement and makes the soil matrix or material hardened. Thus, when soils dry into the adsorption water regime, the small strain shear modulus increases differently than in the capillary water regime, and shows more significant scaling effect compared to the development of finite strain shear modulus in the same regime. In summary, soils containing more clay or greater fines content present stronger effects of capillarity and adsorption, therefore develop higher suction stress and show a higher small strain shear modulus.

Modulus Reduction by Strain Scaling

Once the finite strain and small strain shear moduli for eight soils at various water contents and the information of SWRC and SSCC for each soil is obtained, the ratio G/G_{max} can be fitted by Eq. (5). The fitting results for the three typical soil types (i.e., sandy, silty, and clayey soil) are shown in Fig. 5. The left column [Figs. 5(a–d)] shows the absolute values of the shear modulus at a small shear strain of 0.0001% and at a finite strain of 1%, whereas the right column [Figs. 5(e–h)] shows the normalized shear modulus reduction G/G_{max} curves. Four groups of small strain and finite strain shear moduli at four different water contents for each soil were selected to demonstrate the change of the patterns and shapes of the reduction curves. The shear modulus remains more or less constant when the shear strain is less than 0.005%. Although there are only two points in this fitting process, the shape of the shear modulus reduction curve has been shown to be valid in a range of studies. The shear moduli start to decrease at approximately a shear strain of 0.01%, with the most significant decrease observed between shear strains of 0.01 and 0.3%. As the shear strain increases up to approximately 1%, the shear moduli almost reach their minimum values. Throughout the comparison of three soil types, sandy soil shows a relatively small magnitude of variation for shear modulus as the shear strain increases from 0.0001 to 1%. As the volumetric water content decreases from 0.26 to 0.07, the shear moduli at small strain and finite strain slightly decrease. For silty and clayey soils, the shear modulus at a shear strain of 0.0001% can increase by several orders of magnitude during drying.

The dashed line at $G/G_{max} = 0.5$ in Figs. 5(e–h) reflects the positions of the reference shear strain for each shear modulus reduction curve. Comparing with the counterpart in the left column of Fig. 5, the reduction curves at different water contents almost collapse into one curve, but with slightly different reference strain numbers. As the soil type changes from sandy soil to silty or clayey soil, the reference strain decreases. Specifically, for Esperance sand the reference strains are approximately 0.2% at saturation and slightly increases as soil dries; for Hopi silt the reference shear strains are approximately 0.1% at saturation and the values oscillate back and forth as the soil dries; and for Iowa silt or Denver claystone the reference strains are decreasing as the soils dry, and apparently their reference strains vary in a wider range comparing to those of Hopi silt and Esperance sand. This observation suggests that the reference strain of a certain soil is not always a constant number under unsaturated conditions, and its value varies from soil to soil and changes depending on the volumetric water content and porosity. The collapse of the different reduction curves into one normalized reduction curve from the left to right columns indicates that the coefficient of curvature, m, might be constant for each soil at various volumetric water contents but may alter depending on the soil type.

Correlation between G/G_{max} and SWRC Parameters

The analysis in the previous section leads to an examination of the dependencies of the reference strain, γ_{ref}, and coefficient of curvature, m, on volumetric water content for each soil type. The relationships between reference strain and volumetric water content are shown in Fig. 6(a), whereas the relationships between coefficient of curvature and volumetric water content are shown in Fig. 6(b) for sandy, silty, and clayey soils. The results in Fig. 6 further confirm the intuitive assessment on the characteristics of reference strain and coefficient of curvature and quantifies the dependencies of these two parameters on water content for each soil.

In the case of sandy soils (e.g., Esperance sand), the reference strain is almost one order of magnitude higher than that of the silty and clayey soils. Additionally, Esperance sand exhibits an opposite pattern of evolution with water content comparing to other silty soils and clayey soils. This is possibly related to the suction stress evolution at varying volumetric water content for sandy soil, where suction stress first increases then decreases as the sample dries from saturation. Esperance sand has the largest reference strain at dry condition than at wet condition; whereas Hopi silt and BALT silt show monotonically increases in reference strain with increasing volumetric water content; and claystone presents a larger increment as the volumetric water content increases compared to the other soils. Generally, the reference strain and the volumetric water content are found to be related by a power law relationship, as follows:

$$\gamma_{ref} = \eta \times (\theta^{\xi}) \tag{12}$$

where η = multiplier parameter and ξ = power of water content. These two parameters indicate the range or extent of reference

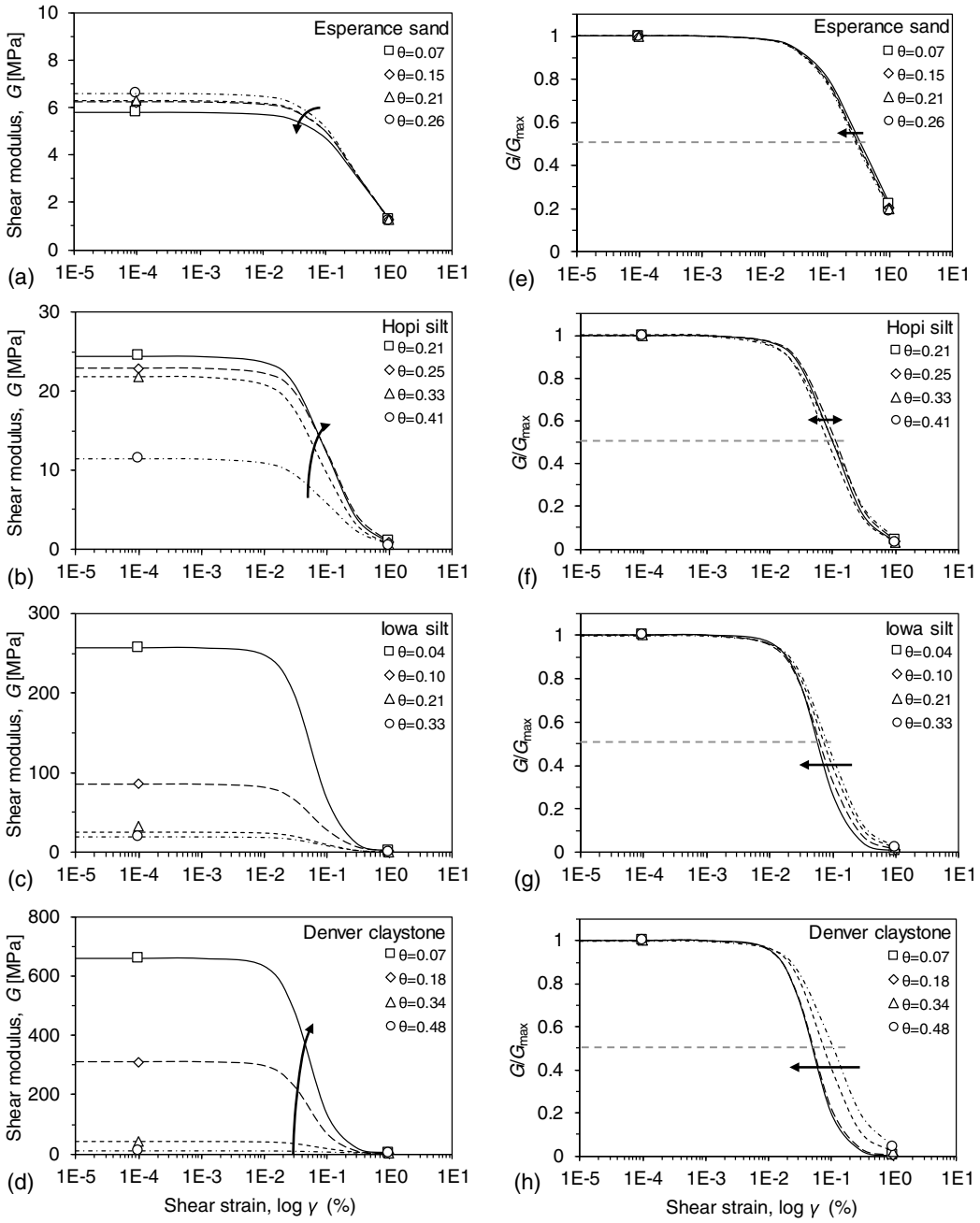

Fig. 5. (a–d) Reduction curves of shear modulus; (e–h) normalized shear modulus at different water contents for different soils; hollow markers are the measured finite-strain and small-strain data; lines are the fitted modulus reduction curves

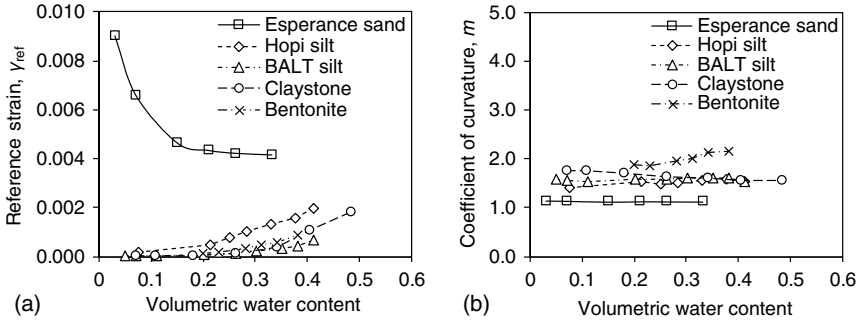

Fig. 6. (a) Relationship with volumetric water content, θ, for reference strain, γ_{ref}; (b) curvature coefficient, m, for three typical sandy, silty, and clayey soils

J. Geotech. Geoenviron. Eng., 2018, 144(2): 04017110

strain variation with water content. The trend lines in Fig. 6(a) show a good fit for each soil with a correlation coefficient, R^2, higher than 0.96.

The relationships between the curvature coefficient, m, and volumetric water content for each selected soil are presented in Figs. 6(b). The values of m are mainly unchanged, indicating that there is no dependency on the volumetric water content for this parameter. The overall number of m ranges from 1.0 to 2.0 for different soils. In light of the evolution of m with θ, for a certain type of soil the curvature coefficient is a constant, but it varies depending on soil type. Accordingly, a mean value was taken for each soil averaging the different volumetric water contents.

After determining the dependency of reference strain on volumetric water content, and the averaged curvature coefficient over various volumetric water contents for each soil, the correlations between parameters ξ, η, and averaged m and the known parameters of the SWRC for each soil are shown in Fig. 7. The parameters of the SWRC model of Lu (2016) were obtained by fitting the measured matric suctions as shown in Fig. 3. The numbers of all fitted parameters are provided in Table 2. The correlations between water content-dependent parameters of reference strain (ξ and η) were investigated over all SWRC parameters (i.e., α, N, $\theta_a^{\max}$, and M). Figs. 7(a and b) show selected correlation between ξ and N, and correlation between ξ and α. Parameter ξ has a strong linear relationship with the pore size distribution parameter, N, although no obvious trend can be found between ξ and other SWRC parameters. Hence, an empirical equation can be used to connect the parameter ξ with the SWRC parameter N, as follows:

$$\xi = -3.0 \times N + 6.9 \tag{13}$$

This equation suggests that a higher N value corresponds to lower ξ value, implying that a more prominent variation of reference strain with volumetric water content occurs in clayey or silty soil with a lower N value, whereas less change in reference strain with volumetric water content occurs in sandy soil with a higher N value. This is consistent with the results shown in Figs. 6(a and b) and 7(a–c).

Similarly, parameter η was investigated by trials of correlating η to all SWRC parameters, and a linear relationship between η and maximum adsorption water, $\theta_a^{\max}$, was observed as shown in Fig. 7(c). An empirical fitting equation is formulated as follows:

$$\eta = 0.10 \times \theta_a^{\max} \tag{14}$$

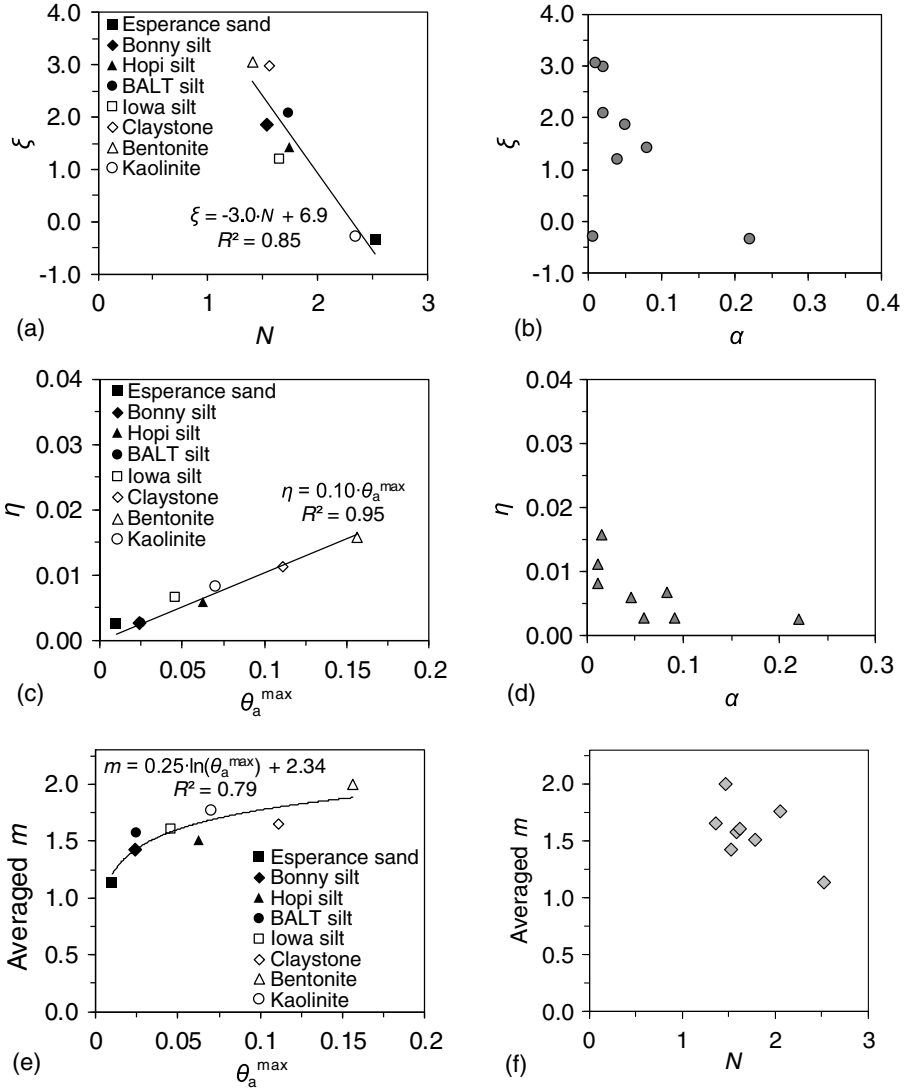

Fig. 7. (a–d) Correlation between the fitting parameters ξ and η of the reference strains and SWRC parameters; (e–f) the correlation between the averaged fitting parameters m of curvature coefficients and Lu (2016) SWRC parameters

J. Geotech. Geoenviron. Eng., 2018, 144(2): 04017110

As an indicator of the reference strain variation, Eq. (14) indicates that parameter η increases linearly with $\theta_a^{\max}$, implying that soils with higher $\theta_a^{\max}$ tend to have a larger variation in the reference strain. Together with the relationship for the parameter ξ, the correlation between η and $\theta_a^{\max}$ leads to the conclusion that silty or clayey soils with higher fines contents will show greater variations in the reference strain as the volumetric water content changes. This also confirms the observations from Figs. 6(a and b) and 7(a–c).

The curvature coefficient, m, can be assumed as a soil-type dependent parameter insensitive to changes in volumetric water content. The correlation between m and the SWRC parameters shows a connection between the extent of shear modulus degradation and the maximum adsorption water content in soil. The correlation observed in Fig. 7(e) can be captured by the following expression:

$$m = 0.25 \times \ln(\theta_a^{\max}) + 2.34 \tag{15}$$

The curvature coefficient shows a logarithmic relationship with increasing maximum adsorption water content. This correlation reveals that the amount of adsorption water in the fines content of a given soil directly influences the degradation rate of shear modulus from small strain to finite strain levels. It also reflects that the higher adsorption water content results in larger difference in orders of magnitude between small strain shear modulus and finite strain shear modulus. This trend, again, proves the contact-force mechanism of the conceptual model that when soil contains more clay content, more significant enhancement of shear modulus prevails at small strain. In the case of zero mean total stress, this enhancement also can be characterized by the evolution in suction stress during drying of a soil (Dong and Lu 2016a).

Prediction and Validation of Shear Modulus

The correlations among the shear modulus reduction parameters (i.e., ξ, η, and m) and the Lu (2016) SWRC model parameters (i.e., N and $\theta_a^{\max}$), provide a convenient approach to estimate either the small strain or finite strain moduli of a soil in the case that one or the other is given and the SWRC of the soil is known. By substituting Eqs. (13) and (14) into Eq. (12), then substituting Eqs. (12) and (15) into Eq. (5), the following predictive equation for the normalized shear modulus reduction curve can be defined:

$$\frac{G}{G_{\max}} = \frac{1}{1 + \left[\frac{\gamma}{\alpha\sigma'(0.10\theta_a^{\max})\cdot\theta^{-3.0n+6.9}}\right]^{0.25\ln(\theta_a^{\max})+2.34}} \tag{16}$$

This equation establishes an approach of determining the normalized shear modulus reduction curve for soils under unsaturated conditions by using empirical correlations based on the SWRC and volumetric water content. Knowing the SWRC information for a certain soil, the small strain shear modulus can be predicted from the finite strain shear modulus, or vice versa. The performance of Eq. (16) is presented in Fig. 8. For predicting small strain or finite strain moduli values, the predicted data points are mainly distributed along the 1:1 diagonal line with small scattering with respect to the measured ones. The R^2 values show a good estimation using the proposed model.

Another validation of the prediction was performed using shear modulus reduction data for three other unsaturated soils available in the literature. The SWRC parameters were obtained by fitting the experimental SWRC measurements of a silty sand from Hoyos et al. (2015), a subgrade soil from Kim et al. (2003), and Ottawa F75 sand from Suprunenko and Ghayoomi (2015), with the SWRC model of Lu (2016), as shown in Figs. 9(a, c, and e), respectively.

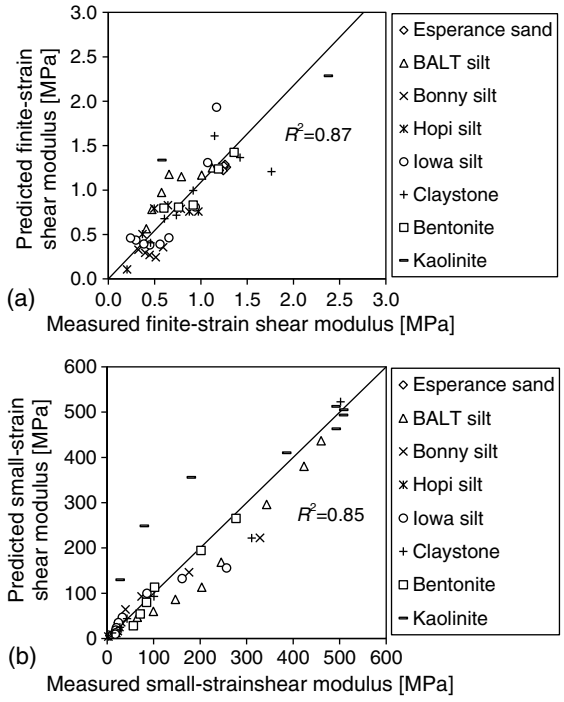

Fig. 8. Prediction of the finite-strain (1%) shear modulus, G_1, using measured small-strain shear modulus and prediction of the small-strain (0.001%) shear modulus, $G_{\max}$, using measured finite-strain shear modulus

The predictions of shear modulus at different strain levels were then compared with experimental data obtained from different cyclic loading tests and resonant column tests, as shown in Figs. 9(b, d, and e). The silty sand samples were tested under a net confining pressure of 25 kPa and two different suction values (a suction of 25 kPa corresponding to a volumetric water content of $\theta = 0.29$, and a suction of 200 kPa corresponding to a volumetric water content of $\theta = 0.17$). The subgrade soil was tested under an effective confining pressure of 41 kPa and various suctions (i.e., 5, 20, 50, 100, and 200 kPa). The Ottawa sand was tested under an effective confining stress of 50 kPa and a suction of 3 kPa. The soils have adsorptive water contents ranging from 0.009 to 0.075, and pore size spectrum parameter N values ranging from 1.436 to 2.525. The predicted curves generally compare well with the measured data points. The different predictions of the shear modulus reduction curves show a good match with the positions of the reference strain, the overall curvature of the degradation curve, and the variation of reduction curve under different suction values. The predicted curves were found to slightly overestimate or underestimate the shear modulus at small and finite strain values, the deviation can be considered acceptable indicating a reliable prediction. Uncertainties may arise from the experimental measurements of resonant column test or torsional shear test. Some extra work measuring a complete SWRC especially in the high suction range is necessary to obtain good predictions of the shear modulus reduction.

Summary and Conclusions

In this study, the small strain shear moduli and finite strain shear moduli were compared to evaluate the different mechanisms governing the shear modulus reduction with increasing shear strain

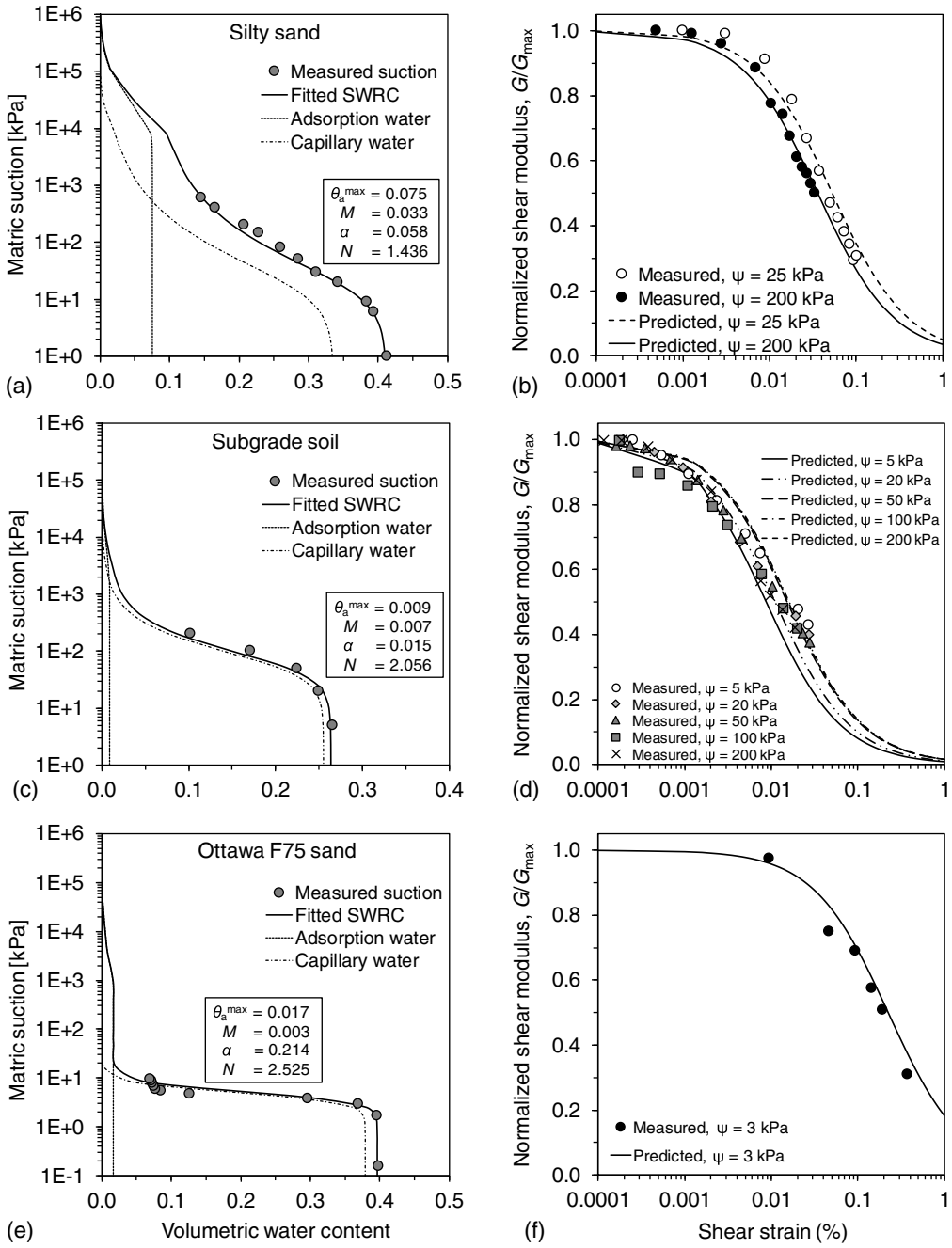

Fig. 9. Measured SWRC with fitted Lu (2016) model and comparisons of measured shear modulus reduction with model prediction for: (a and b) silty sand (data from Hoyos et al. 2015; L. Hoyos, personal communication, 2016); (c and d) subgrade soil (data from Kim et al. 2003); (e and f) Ottawa sand (data from Suprunenko and Ghayoomi 2015)

amplitude. It was found that the shear modulus at finite strains is controlled by the soil structure, whereas the shear modulus at small strains is controlled by interparticle contact forces associated with the pore water in the capillarity or adsorption regimes. The SWRC model of Lu (2016) clearly distinguishes between the capillary and adsorption soil water regimes, which helped to better interpret the impacts of soil type and volumetric water content on the shear modulus reduction curve.

Using the results from tests on eight different soil types (ranging from sandy, silty, to clayey soils), a new shear modulus reduction curve was established to take into consideration the dependency of water content and the effect of soil water adsorption. Relationships between key parameters of this model, the reference strain and curvature coefficient, were defined based on the results from the experimental testing program. The reference strain was found to be in a power law relationship with water content for a certain soil, with a magnitude varying from soil to soil. The curvature coefficient is soil-type dependent and was not as sensitive to the volumetric water content. Using the SWRC model of Lu (2016), the reference strain was correlated with the maximum adsorption water content and the pore spectrum indicator of the SWRC. The curvature coefficient reflected the effect of soil water hydration, and is found to be correlated with soil water adsorption. The proposed prediction approach provides a simple and convenient equation to estimate either small strain or finite strain shear modulus by knowing one or the other and the information of soil water

retention. It also can be used to calculate the shear modulus of a soil at any given strain level by knowing the SWRC and the maximum shear modulus.

Acknowledgments

This research is supported by a grant from the National Science Foundation (NSF) [Civil, Mechanical and Manufacturing Innovation (CMMI)-1230544]. The authors also would like to thank L. Hoyos of the University of Texas at Arlington for the private correspondence regarding the unpublished experimental data.

References

Alramahi, B., Alshibli, K., Fratta, D., and Trautwein, S. (2008). "A suction-control apparatus for the measurement of p and s-wave velocity in soils." *Geotech. Test. J.*, 31(1), 471.

Atkinson, J. H. (2000). "Non-linear soil stiffness in routine design." *Géotechnique*, 50(5), 487–508.

Borden, R. H., Shao, L., and Gupta, A. (1996). "Dynamic properties of Piedmont residual soils." *J. Geotech. Eng.*, 10.1061/(ASCE)0733-9410(1996)122:10(813), 813–821.

Clayton, C. R. I. (2011). "Stiffness at small strain: Research and practice." *Géotechnique*, 61(1), 5–37.

Darendeli, M. B. (1997). "Dynamic properties of soils subjected to 1994 Northridge earthquake." M.S. thesis, Univ. of Texas at Austin, Austin, TX.

Darendeli, M. B. (2001). "Development of a new family of normalized modulus reduction and material damping curves." Ph.D. thesis, Univ. of Texas at Austin, Austin, TX.

Dong, Y., and Lu, N. (2016a). "Correlation between small strain shear modulus and suction stress of unsaturated soils in capillary regime." *J. Geotech. Geoenviron. Eng.*, 10.1061/(ASCE)GT.1943-5606.0001531, 04016039.

Dong, Y., and Lu, N. (2016b). "Dependencies of shear wave velocity and shear modulus of soil on saturation." *J. Eng. Mech.*, 10.1061/(ASCE)EM.1943-7889.0001147, 04016083.

Dong, Y., Lu, N., and McCartney, J. S. (2016). "Unified model for small-strain shear modulus of variably saturated soil." *J. Geotech. Geoenviron. Eng.*, 10.1061/(ASCE)GT.1943-5606.0001506, 04016039.

Frydman, S., and Baker, R. (2009). "Theoretical soil-water characteristic curves based on adsorption, cavitation, and a double porosity model." *Int. J. Geomech.*, 10.1061/(ASCE)1532-3641(2009)9:6(250), 250–257.

Hardin, B. O., and Drnevich, V. P. (1972a). "Shear modulus and damping in soils: Design equations and curves." *J. Soil Mech. Found. Div*, 98(SM7), 667–692.

Hardin, B. O., and Drnevich, V. P. (1972b). "Shear modulus and damping in soils: Measurement and parameter effects." *J. Soil Mech. Found. Div.*, 98(SM6), 603–624.

Hoyos, L. R., Suescún-Florez, E. A., and Puppala, A. J. (2015). "Stiffness of intermediate unsaturated soil from simultaneous suction-controlled resonant column and bender element testing." *Eng. Geol.*, 188(7), 10–28.

Idriss, I. M. (1990). "Response of soft soil sites during earthquakes." *Proc., H. Bolten Seed Memorial Symp.*, Vol. 2, BiTech Publishers, Vancouver, Canada, 273–298.

Ishibashi, I., and Zhang, X. (1993). "Unified dynamic shear moduli and damping ratio of sand and clay." *Soil. Found.*, 33(1), 182–191.

Iwasaki, T., Tatsuoka, F., and Takagi, Y. (1978). "Shear moduli of sands under cyclic torsional shear loading." *Soil. Found.*, 18(1), 39–56.

Khosravi, A., and McCartney, J. S. (2012). "Impact of hydraulic hysteresis on the small-strain shear modulus of low plasticity soils." *J. Geotech. Geoenviron. Eng.*, 10.1061/(ASCE)GT.1943-5606.0000713, 1326–1333.

Kim, D. S., Seo, W. S., and Kim, M. J. (2003). "Deformation characteristics of soils with variations of capillary pressure and water content." *Soil. Found.*, 43(4), 71–79.

Kokusho, T. (1980). "Cyclic triaxial test of dynamic soil properties for wide strain range." *Soil. Found.*, 20(2), 45–60.

Kramer, S. L. (1996). *Geotechnical earthquake engineering*, Prentice Hall, Upper Saddle River, NJ.

Likitlersuang, S., Teachavorasinskun, S., Surarak, C., Oh, E., and Balasubramaniam, A. (2013). "Small strain stiffness and stiffness degradation curve of Bangkok clays." *Soil. Found.*, 53(4), 498–509.

Likos, W. J., Lu, N., and Wenszel, W. (2011). "Performance of a dynamic dew point method for moisture isotherms of clays." *Geotech. Test. J.*, 34(4), 373–382.

Lu, N. (2016). "Generalized soil water retention equation for adsorption and capillarity." *J. Geotech. Geoenviron. Eng.*, 10.1061/(ASCE)GT.1943-5606.0001524, 04016051.

Lu, N., Godt, J., and Wu, D. (2010). "A closed form equation for effective stress in variably saturated soil." *Water Resour. Res.*, 46(5), W05515.

Lu, N., and Kaya, M. (2013). "A drying cake method for measuring suction-stress characteristic curve, soil-water-retention curve, and hydraulic conductivity function." *Geotech. Test. J.*, 36(1), 1–19.

Lu, N., and Kaya, M. (2014). "Power law for elastic moduli of unsaturated soil." *J. Geotech. Geoenviron. Eng.*, 10.1061/(ASCE)GT.1943-5606.0000990, 46–56.

Lu, N., and Khorshidi, M. (2015). "Mechanism for soil-water retention and hysteresis at high suction range." *J. Geotech. Geoenviron. Eng.*, 10.1061/(ASCE)GT.1943-5606.0001325, 04015032.

Lu, N., and Likos, W. J. (2004). *Unsaturated soil mechanics*, Wiley, Hoboken, NJ.

Lu, N., and Likos, W. J. (2006). "Suction stress characteristic curve for unsaturated soils." *J. Geotech. Geoenviron. Eng.*, 10.1061/(ASCE)1090-0241(2006)132:2(131), 131–142.

Or, D., and Tuller, M. (1999). "Liquid retention and interfacial area in variably saturated porous media: Upscaling from single-pore to sample-scale model." *Water Resour. Res.*, 35(12), 3591–3605.

Rampello, S., Viggiani, G. M. B., and Amorosi, A. (1997). "Small-strain stiffness of reconstituted clay compressed along constant triaxial effective stress ratio paths." *Géotechnique*, 47(3), 475–489.

Revil, A., and Lu, N. (2013). "Unified water sorption and desorption isotherms for clayey porous materials." *Water Resour. Res.*, 49(9), 5685–5699.

Santamarina, J. C., Klein, K. A., and Fam, M. A. (2001). *Soils and waves: Particulate materials behavior, characterization and process monitoring*, Wiley, Chichester, U.K.

Seed, H. B., Wong, R. T., Idriss, I. M., and Tokimatsu, K. (1986). "Moduli and damping factors for dynamic analyses of cohesionless soils." *J. Geotech. Eng.*, 10.1061/(ASCE)0733-9410(1986)112:11(1016), 1016–1032.

Suprunenko, G., and Ghayoomi, M. (2015). "Suction-controlled cyclic triaxial system for measurement of dynamic properties of unsaturated soils." *15th Pan-American Conf. on Soil Mechanics and Geotechnical Engineering*, IOS Press, Amsterdam, Netherlands, 2150–2157.

Tuller, M., Or, D., and Dudley, L. M. (1999). "Adsorption and capillary condensation in porous media-liquid retention and interfacial configurations in angular pores." *Water Resour. Res.*, 35(7), 1949–1964.

van Genuchten, M. T. (1980). "A closed-form equation for predicting the hydraulic conductivity of unsaturated soils." *Soil Sci. Soc. Am. J.*, 44(5), 892–898.

Viggiani, G., and Atkinson, J. H. (1995). "Stiffness of fine-grained soil at very small strains." *Géotechnique*, 45(2), 249–265.

Vucetic, M., and Dobry, R. (1991). "Effect of soil plasticity on cyclic response." *J. Geotech. Eng.*, 10.1061/(ASCE)0733-9410(1991)117:1(89), 89–107.

Wayllace, A., and Lu, N. (2012). "A transient water release and imbibitions method for rapidly measuring wetting and drying soil water retention and hydraulic conductivity functions." *Geotech. Test. J.*, 35(1), 103–117.

Yang, J., and Gu, X. Q. (2013). "Shear stiffness of granular material at small strains: Does it depend on grain size?" *Géotechnique*, 63(2), 165–179.

Yokota, K., Imai, T., and Konno, M. (1981). "Dynamic deformation characteristics of soils determined by laboratory tests." *OYO Technical Rep.*, 3, 13–37.